IOP PUBLISHING JOURNAL OF PHYSICS D: APPLIED PHYSICS

J. Phys. D: Appl. Phys. **42** (2009) 025205 (10pp) doi:10.1088/0022-3727/42/2/025205

PIC simulations of the separate control of ion flux and energy in CCRF discharges via the electrical asymmetry effect

Z Donkó[1], J Schulze[2], B G Heil[2,3] and U Czarnetzki[2]

[1] Research Institute for Solid State Physics and Optics of the Hungarian Academy of Science, Budapest, Hungary

[2] Institute for Plasma and Atomic Physics, Ruhr-University, Bochum, Germany

E-mail: fjschulze@hotmail.com

Received 6 August 2008, in final form 12 November 2008
Published 18 December 2008
Online at stacks.iop.org/JPhysD/42/025205

Abstract

Recently a novel approach for achieving separate control of ion flux and energy in capacitively coupled radio frequency (CCRF) discharges based on the electrical asymmetry effect (EAE) was proposed (Heil *et al* 2008 *J. Phys. D: Appl. Phys.* **41** 165202). If the applied, temporally symmetric voltage waveform contains an even harmonic of the fundamental frequency, the sheaths in front of the two electrodes are necessarily asymmetric. A dc self-bias develops and is a function of the phase angle between the driving voltages. By tuning the phase, precise and convenient control of the ion energy can be achieved while the ion flux stays constant. This effect works even in geometrically symmetric discharges and the role of the two electrodes can be reversed electrically. In this work the EAE is verified using a particle in cell simulation of a geometrically symmetric dual-frequency CCRF discharge operated at 13.56 and 27.12 MHz. The self-bias is a nearly linear function of the phase angle. It is shown explicitly that the ion flux stays constant within ±5%, while the self-bias reaches values of up to 80% of the applied voltage amplitude and the maximum ion energy is changed by a factor of 3 for a set of low pressure discharge conditions investigated. The EAE is investigated at different pressures and electrode gaps. As geometrically symmetric discharges can be made electrically asymmetric via the EAE, the plasma series resonance effect is observed for the first time in simulations of a geometrically symmetric discharge.

(Some figures in this article are in colour only in the electronic version)

1. Introduction

Capacitively coupled radio frequency (CCRF) discharges are often used for industrial processes such as etching and deposition processes for semiconductor fabrication (chip production, solar cells, etc). For these applications separate control of the ion flux and the ion energy is essential. The ion flux determines the throughput of the process and the ion energy controls the etching and deposition processes taking place at the wafer's surface [2].

Separate control of ion flux and ion energy cannot be achieved in conventional single frequency discharges, since both parameters are controlled by the amplitude of the applied voltage amplitude [3–34].

Besides hybrid discharges [35] the usual method to overcome this problem is the use of dual-frequency CCRF discharges operated at two substantially different frequencies applied to one or more electrodes [20, 36–47] with a low frequency voltage that is much higher than the high frequency voltage. Typically such discharges are operated at 2 and 27 MHz. The ion flux is assumed to be mainly controlled by the high frequency component, since electron heating is more efficient at higher frequencies. Due to the higher voltage the ion energy is assumed to be mainly controlled by the low frequency component. However, recent investigations have shown that there can be a strong coupling between the two

[3] Current address: Richardt Patents and Trademarks, Leergasse 11, D-65343 Eltville am Rhein, Germany.

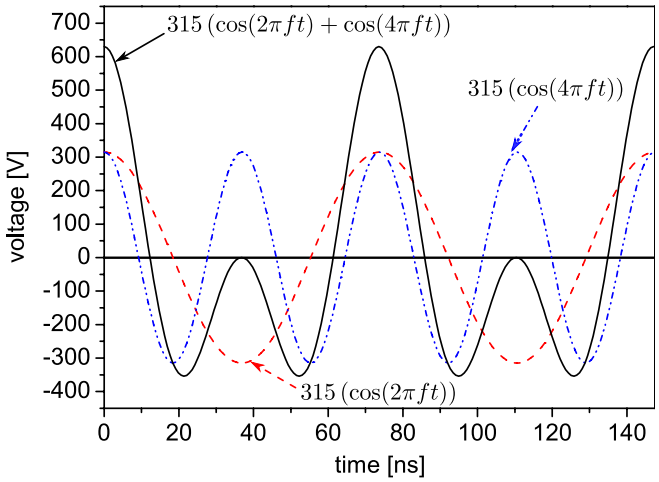

Figure 1. Voltage waveform $V_{AC}(t) = 315(\cos(2\pi ft) + \cos(4\pi ft))$, where $f = 13.56$ MHz, applied to the discharge for two RF periods (solid black line). The absolute values of the positive and negative extremes and the voltages across the two sheaths are different. Therefore, a dc self-bias develops under these conditions.

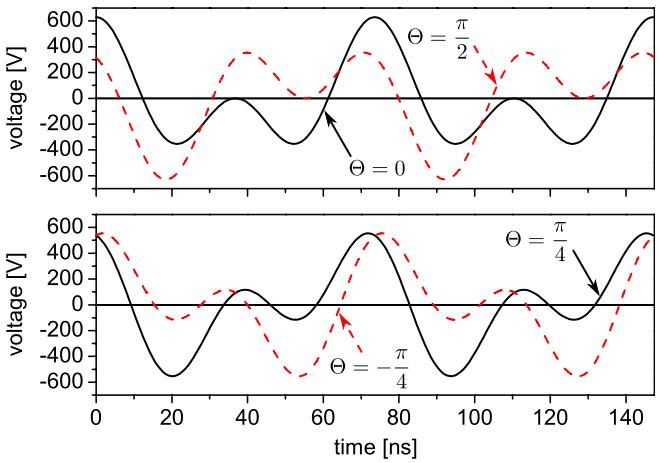

Figure 2. $V_{AC}(t) = 315(\cos(2\pi ft + \Theta) + \cos(4\pi ft))$ for different values of the phase angle Θ [1, 23].

frequencies, which might limit the separate control of ion flux and energy [20, 41–46].

Recently a novel concept to solve this problem was introduced and is based on the newly discovered electrical asymmetry effect (EAE) in dual-frequency CCRF discharges [1, 23]. The EAE was analysed in detail using an analytical model and a fluid simulation [1]. A consequence of the EAE is the generation of a dc self-bias even in geometrically symmetric CCRF discharges. In geometrically asymmetric discharges a dc self-bias is generated naturally because of the different electrode sizes and develops in order to compensate electron and ion flux to each electrode within one RF period. In geometrically symmetric discharges with equal electrode sizes a dc self-bias is generated if the absolute values of the positive and negative extremes of the applied RF voltage waveform are different [1]. This can be achieved by applying a fundamental and an even harmonic to the discharge and by controlling the phase between the two voltage waveforms. By changing the phase angle, the symmetry of the applied voltage waveform can be changed from symmetric (strong dc self-bias) to anti-symmetric (no dc self-bias) and vice versa. The effect is maximized if the second harmonic of the fundamental is applied to the discharge additionally, but generally works, if the applied voltage waveform contains any even harmonic of its fundamental frequency. A detailed description of this symmetry consideration and the EAE is given elsewhere [1]. Here only a short graphical explanation is presented.

Figure 1 shows graphically why adding a second harmonic and choosing the right phase between the fundamental and the even harmonic ($\Theta = 0^\circ$ in figure 1) results in asymmetric sheaths and a dc self-bias even in a geometrically symmetric discharge. In this figure, the voltage waveform

$$V_{AC}(t) = 315(\cos(2\pi ft) + \cos(4\pi ft)) \tag{1}$$

is plotted, where $f = 13.56$ MHz. V_{AC} is considered to be the ac voltage applied to a discharge. Each of the two cosine functions is harmonically symmetric ($\tilde{\phi}(\varphi + \pi) = -\tilde{\phi}(\varphi)$, $\varphi = \omega t$, $\tilde{\phi}$ corresponds to the applied voltage), but the sum of the two is not. The sum is symmetric with respect to $\varphi = \pi$ ($\tilde{\phi}(\varphi) = \tilde{\phi}(-\varphi)$). The absolute values of the positive and negative extremes are different.

According to equations (20) and (22) in [1] the dc self-bias η is determined by the absolute extremes of the applied voltage waveform, $\tilde{\phi}_{m1}$ and $\tilde{\phi}_{m2}$, and the symmetry parameter ε:

$$\eta = -\frac{\tilde{\phi}_{m1} + \varepsilon\tilde{\phi}_{m2}}{1 + \varepsilon}, \tag{2}$$

$$\varepsilon = \left|\frac{\hat{\phi}_{sg}}{\hat{\phi}_{sp}}\right| = \left(\frac{A_p}{A_g}\right)^2 \frac{\bar{n}_{sp}}{\bar{n}_{sg}} \frac{I_{sg}}{I_{sp}}. \tag{3}$$

Here A_p and A_g are the areas of the powered and grounded electrode, respectively. $\hat{\phi}_{sp}$ and $\hat{\phi}_{sg}$ are the maximum sheath voltages, $\bar{n}_{sp}$, $\bar{n}_{sg}$ correspond to the mean ion densities and I_{sp} and I_{sg} are the so-called sheath integrals for the respective sheath [1]:

$$I_s = 2\int_0^1 p_s(\xi)\xi \, d\xi \tag{4}$$

with $\xi = x/s_m$ and $p_s(\xi) = n_i(x)/\bar{n}_i$. Here s_m is the maximum sheath width and n_i is the ion density.

According to [1] the ratio of the sheath integrals in equation (3) is assumed to be unity. This assumption will be verified in this paper. Therefore, in a geometrically symmetric discharge ($A_p/A_g = 1$) the symmetry parameter only depends on the ratio of the mean ion densities in the sheaths.

Based on equation (2) it is obvious that the dc self-bias can be changed by changing the difference between the absolute positive and negative extremes of the applied voltage waveform. This can be achieved by changing the phase between the fundamental and the even harmonic. Figure 2 shows plots of the function:

$$V_{AC}(t) = V_0(\cos(2\pi ft + \Theta) + \cos(4\pi ft)), \tag{5}$$

where $f = 13.56$ MHz and $V_0 = 315$ V. At $\Theta = 0$ and $\Theta = \pi/2$ the applied voltage waveform is symmetric and

the difference between the absolute values of the positive and negative extremes is maximum. Following equation (2) this difference leads to the generation of a strong dc self-bias even if $\varepsilon = 1$ is assumed. At the phases $\Theta = -\pi/4$ and $\Theta = \pi/4$ the applied voltage waveform is anti-symmetric and the absolute values of the positive and negative extremes are the same. Therefore, the dc self-bias is expected to be minimum for these phase angles. The voltage waveforms in figures 1 and 2 are ac voltages and do not include the dc self-bias. If there is a dc self-bias, the sheath voltages and, consequently, also the sheath densities will be different. This leads to a symmetry parameter different from unity, which causes an even stronger dc self-bias. Therefore, the EAE is self-amplifying.

The phase can be used to adjust the symmetry of the applied voltage waveform and the dc self-bias. Additionally, looking at phases $\Theta = 0$ and $\Theta = \pi/2$ it is obvious that by simply changing the phase angle the roles of the two electrodes can be reversed electrically. In contrast to conventional dual-frequency CCRF discharges operated at large frequency differences the EAE is strongest if the frequency difference is small, i.e. if the second harmonic of the fundamental is used. A great advantage of the EAE for industrial applications is the easy control of the dc self-bias and, consequently, the ion energy by changing the phase between the applied frequencies in both geometrically symmetric and asymmetric discharges. This is in great contrast to the conventional dc self-bias effect which relies on the geometry of the discharge and is not reversible.

In this paper the EAE is investigated by a self-consistent particle in cell (PIC) simulation. The results obtained by a non-self-consistent fluid simulation and an analytical model [1] are verified. It is shown that the dc self-bias is a nearly linear function of the phase between the applied voltage waveforms as predicted before. The effect of the variation of the self-bias by the EAE on the ion flux-energy distribution function is investigated and the results are compared with the investigations performed before. Furthermore, it is shown that the separate control of ion energy and ion flux can indeed be achieved using this technique. In contrast to the non-self-consistent fluid simulation and the analytical model used before [1] the self-consistent PIC simulation yields both the ion flux-energy distribution and the plasma density. Effects on the excitation dynamics are also investigated. Finally, the EAE is examined at different pressures and electrode gaps.

The paper is structured in the following way: in section 2 the PIC simulation and the method used to determine the dc self-bias in the simulation are briefly described. In section 3 the results are presented. This section is divided into two parts. The first part focuses on the scenario previously investigated by the analytical model and the fluid simulation. Here the results obtained from the PIC simulation are directly compared with the results of [1] and additional investigations on the separate control of ion flux and energy are performed. In the second part, a broader parameter range is investigated using the PIC simulation. The pressure and the electrode gap are varied and the effect on various plasma parameters is discussed with a focus on the EAE and separate control of the ion flux and energy. Finally, conclusions are drawn in section 4.

2. PIC simulation

We describe CCRF discharges in argon using a one-dimensional (1d3v) bounded plasma PIC simulation code, complemented with a Monte Carlo treatment of collision processes (PIC/MCC [20, 48, 49]). The electrodes are assumed to be infinite, planar and parallel. In our implementation of the PIC simulation, one of the electrodes is driven by a voltage specified by equation (5), while the other electrode is grounded. The electron impact cross sections for the collision processes are taken from [50]. For the positive ions, elastic collisions with the gas atoms are divided into an isotropic and a backward part [51]. The cross sections for these collisions are taken from [51, 52]. Metastable atoms are not taken into account. The bias voltage η is determined in the simulation in an iterative way to ensure that the charged particle fluxes to the two electrodes averaged over one low frequency RF period become equal. Electrons are reflected from the electrode surfaces with a probability of 0.2 and the secondary electron emission coefficient is taken to be $\gamma = 0.1$ for most of our simulations. The number of superparticles in the simulations is of the order of 10^5. From the trajectories of the particles followed in the PIC simulation as well as from the collision events we derive the spatio-temporal distributions of several discharge characteristics (e.g. potential, densities, electron heating, ionization and excitation rates).

3. Results

First we focus on the scenario investigated previously by a fluid simulation and an analytical model [1] and direct comparisons between PIC and those previously obtained results are performed. In the second part a more general investigation of the EAE and its effects on the ion energy and flux at different pressures and electrode gaps is performed.

3.1. Results at 20 mTorr with a 6.7 cm electrode gap

The conditions investigated here correspond to a geometrically symmetric dual frequency discharge operated in argon at 13.56 and 27.12 MHz at 20 mTorr with an electrode gap of $d = 6.7$ cm, similar to conditions of an experimental investigation by Godyak and Piejak in a single frequency CCRF discharge [18, 19, 21, 23, 53, 54]. A voltage waveform V_{AC} with the shape specified by equation (5) and with an amplitude $V_0 = 315$ V is applied to the discharge. A neutral gas temperature $T_g = 350$ K, a secondary electron emission coefficient $\gamma = 0.1$ and an electron reflection coefficient $\alpha = 0.2$ are used.

Figure 3 shows the voltages across the sheaths at the powered electrode (V_{sp}) and at the grounded electrode (V_{sg}) as well as the total voltage across the discharge (V_{total}) according to equation (6) (solid black line) at $\Theta = 0^\circ$ within one low frequency ($1\,\omega$) RF period. A dc self-bias $\eta = 213$ V builds up at this phase angle. These voltages agree well with those resulting from model calculations performed before (figure 11 in [1]). In the analytical model of [1] the total voltage across the discharge is assumed to be the sum of the voltages across both sheaths:

$$V_{total} = V_{sp} + V_{sg}. \quad (6)$$

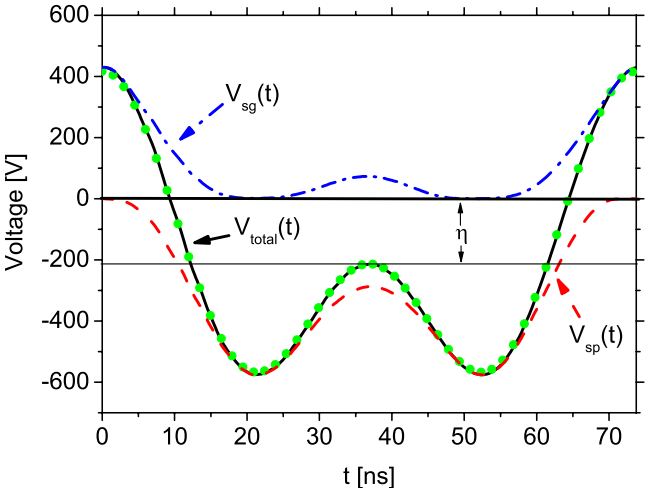

Figure 3. Total voltage across the discharge, $V_{\text{total}} = V_{\text{AC}} + \eta$, (circles) and sum of both sheath voltages (solid line), voltage across the sheath at the powered electrode, V_{sp}, (dashed line) voltage across the sheath at the grounded electrode, V_{sg}, (dashed-dotted line) and dc self-bias, η, as they result from the PIC simulation at $\Theta = 0^\circ$. The results agree well with model calculations performed before [1].

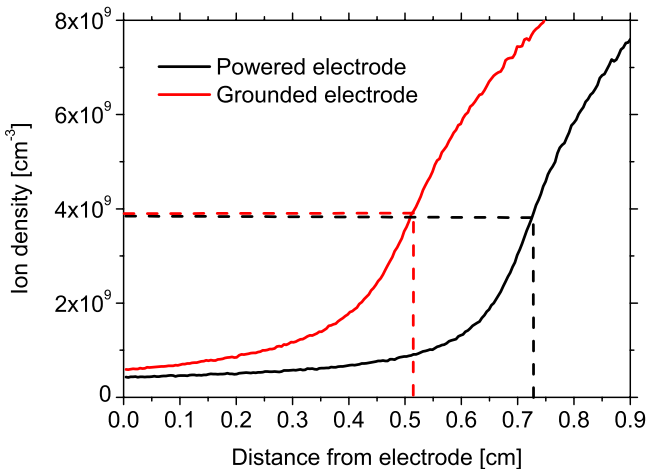

Figure 4. Time averaged ion density profiles in front of each electrode at $\Theta = 0^\circ$. The dashed lines show the maximum sheath edge at each electrode within one lf RF period calculated by equation (8).

The total voltage across the discharge is the sum of the applied voltage, V_{AC}, and the dc self-bias, η:

$$V_{\text{total}} = V_{\text{AC}} + \eta. \tag{7}$$

Figure 3 shows that the assumption corresponding to equation (6) is correct under the conditions investigated here: at the low pressure of 20 mTorr, the voltage drop across the plasma bulk is negligible and the total voltage across the discharge is indeed the sum of both sheath voltages.

Figure 4 shows the ion density profiles in front of each electrode as calculated by the PIC simulation when $\Theta = 0^\circ$. The dashed lines correspond to the maximum sheath edge at the respective electrode within one period of the fundamental frequency calculated based on the following

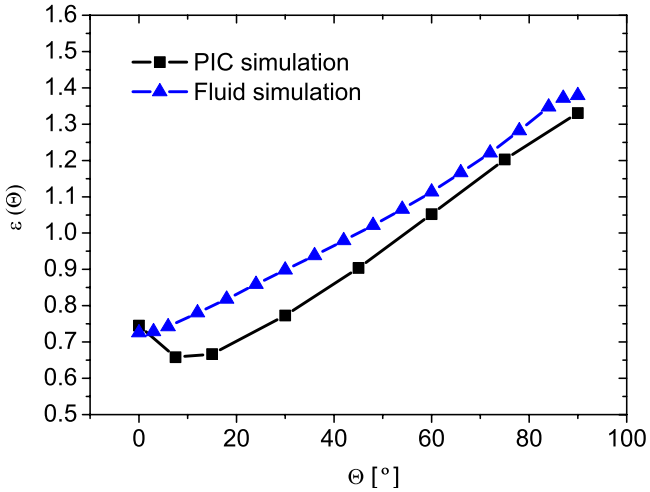

Figure 5. Symmetry parameter defined by equation (3) as a function of the phase angle Θ (black line (squares)—PIC simulation, blue line (triangles)—fluid simulation [1]).

criterion introduced by Brinkmann [55]:

$$\int_0^s n_{\text{e}}(x)\,\mathrm{d}x = \int_s^{d/2} (n_{\text{i}} - n_{\text{e}})\,\mathrm{d}x. \tag{8}$$

Here s is the formal sheath edge, n_{e} is the electron density, n_{i} is the ion density and the x-direction is perpendicular to the electrodes.

Figure 4 clearly shows that the maximum sheath widths at each electrode are different and that the discharge is therefore asymmetric, although the reactor geometry is symmetric. The asymmetry of a discharge can be characterized via the so-called symmetry parameter ε defined by equation (3). In the analytical model of [1] the ratio of the sheath integrals is assumed to be unity. The PIC simulation verifies this assumption at all phase angles investigated. Therefore, as a good approximation the symmetry parameter in a geometrically symmetric discharge ($A_{\text{p}}/A_{\text{g}} = 1$) only depends on the ratio of the mean ion densities in the respective sheath:

$$\varepsilon = \frac{\bar{n}_{\text{sp}}}{\bar{n}_{\text{sg}}}. \tag{9}$$

The symmetry of the applied voltage waveform can be changed by changing the phase angle Θ. This leads to different absolute values of the positive and negative extremes of the applied voltage and, therefore, to a dc self-bias varying with the phase angle between the two harmonics. A finite bias leads to different sheath voltages, which then lead to different sheath densities. Different sheath densities cause the symmetry parameter ε to deviate from unity. This yields an even stronger self-bias and self-amplifies the effect. Figure 5 shows the symmetry parameter ε as a function of Θ calculated by the PIC simulation and the fluid simulation of [1]. The symmetry parameter is a nearly linear function of the phase angle. Small deviations between PIC and fluid simulation are found. The minimum of ε calculated by the PIC simulation at $\Theta = 7.5^\circ$ is a consequence of a slight change in the ratio of

the sheath integrals and is not related to a change in the ratio of the mean ion densities in the sheath.

Figure 6 shows the effect of a variation of the phase angle Θ in equation (5) on the dc self-bias η as it results from the PIC simulation, as well as from the fluid simulation and from the analytical model of the EAE [1]. The self-consistent PIC simulation verifies the result of the models: the dc self-bias is a nearly linear function of the phase angle between the applied frequencies. The results from the fluid simulation and the analytical model on the one hand and the PIC simulation on the other hand are basically identical. Nevertheless, both curves differ by a small phase shift of about 7°. While the fluid simulation confirms the analytical prediction that extremes of the bias are reached at phase angles of 0° and 90°, respectively, the PIC simulation finds extremes at 7.5° and 97.5°. One might suspect that some kinetic effect is responsible for this difference.

Figure 7 shows the effect of varying the phase angle Θ of equation (5) on the ion flux-energy distribution at each electrode. By changing Θ from 0° to 90° the maximum ion energy at each electrode can be changed by a factor of about 3. Furthermore, the role of each electrode can be reversed. Figure 7 agrees well with the distribution functions reported in [1]. The local maxima of the distribution functions at low energies are caused by ions, which undergo charge exchange collisions in the sheath.

The left plot of figure 8 shows the ion flux at both electrodes as the phase angle Θ is varied from 0° to 90°. The ion flux is constant within ±5%, while the maximum ion energy changes by a factor of 3 as Θ changes (see figure 7). The observed stability of the ion flux is within the range of tolerance for most industrial applications [56, 57]. The right plot of figure 8 shows the ion density in the discharge centre calculated by the PIC simulation. The ion density is basically constant as the phase angle changes. Based on the above results this technique easily allows separate control of ion energy and ion flux by keeping the applied voltage constant and changing the phase angle Θ.

Figure 9 shows the space and phase resolved power density dissipated to electrons and ions when $\Theta = 0°$ and $\Theta = 90°$. The power density dissipated to electrons and ions $p_{e,i}$ is defined as

$$p_{e,i} = \vec{j}_{e,i} \cdot \vec{E}. \tag{10}$$

Here $\vec{j}_{e,i}$ is the current density of the respective particle species and $\vec{E}$ is the electric field. Again the asymmetry of the discharge due to the EAE is obvious. At $\Theta = 0°$ most power dissipation takes place at the bottom powered electrode. At $\Theta = 90°$, the role of the electrodes is reversed via the EAE and most power dissipation takes place at the top grounded electrode. Electrons are accelerated at the sheath edge by the expanding sheath at both electrodes. The high frequency oscillations of the power density dissipated to the electrons during the initial sheath expansion at the powered electrode at $\Theta = 0°$ (0–20 ns) and at the grounded electrode at $\Theta = 90°$ (20–40 ns) are caused by the plasma series resonance (PSR) effect [10–23]. Here the PSR effect is observed in a geometrically symmetric discharge for the first time. The PSR effect is caused by the non-linear charge voltage relation of the sheath in a capacitive discharge. In a completely symmetric discharge the non-linearities of both sheaths cancel

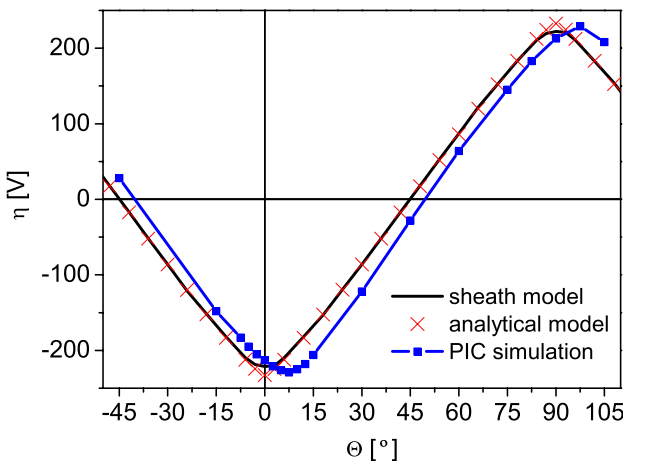

Figure 6. Dc self-bias η calculated by the Brinkmann sheath model (solid black line [1]), the analytical model (crosses, [1]) and the PIC simulation (squares and solid line).

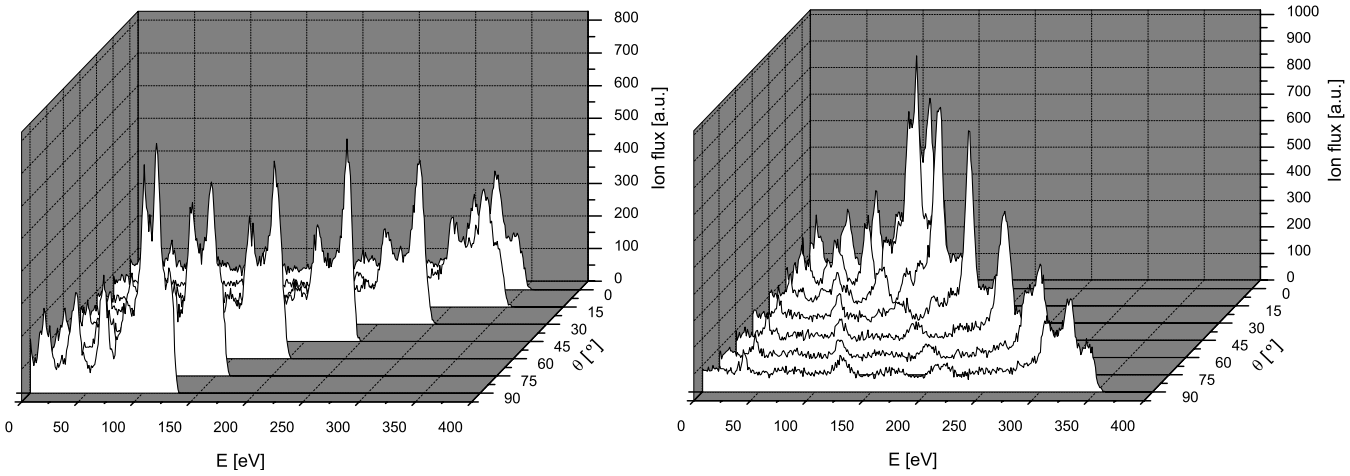

Figure 7. Ion flux–energy distributions at the powered (left) and grounded (right) electrode as a function of the phase angle Θ of equation (5) calculated by the PIC simulation under the conditions mentioned in the text.

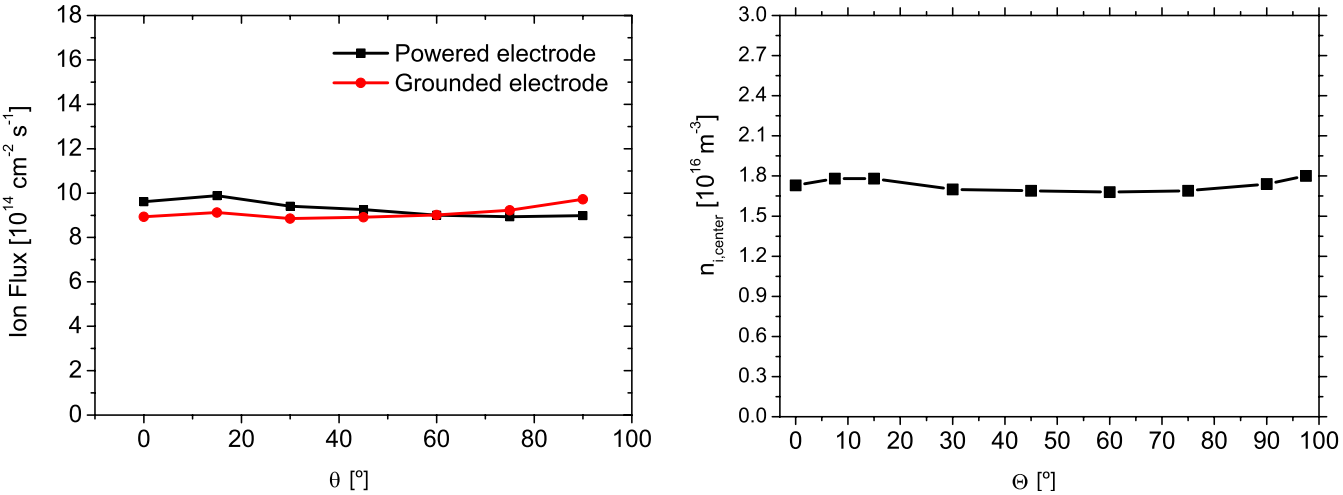

Figure 8. Left: ion fluxes at the powered and grounded electrode as a function of the phase angle Θ in equation (5). Right: ion density in the discharge centre as a function of the phase angle Θ.

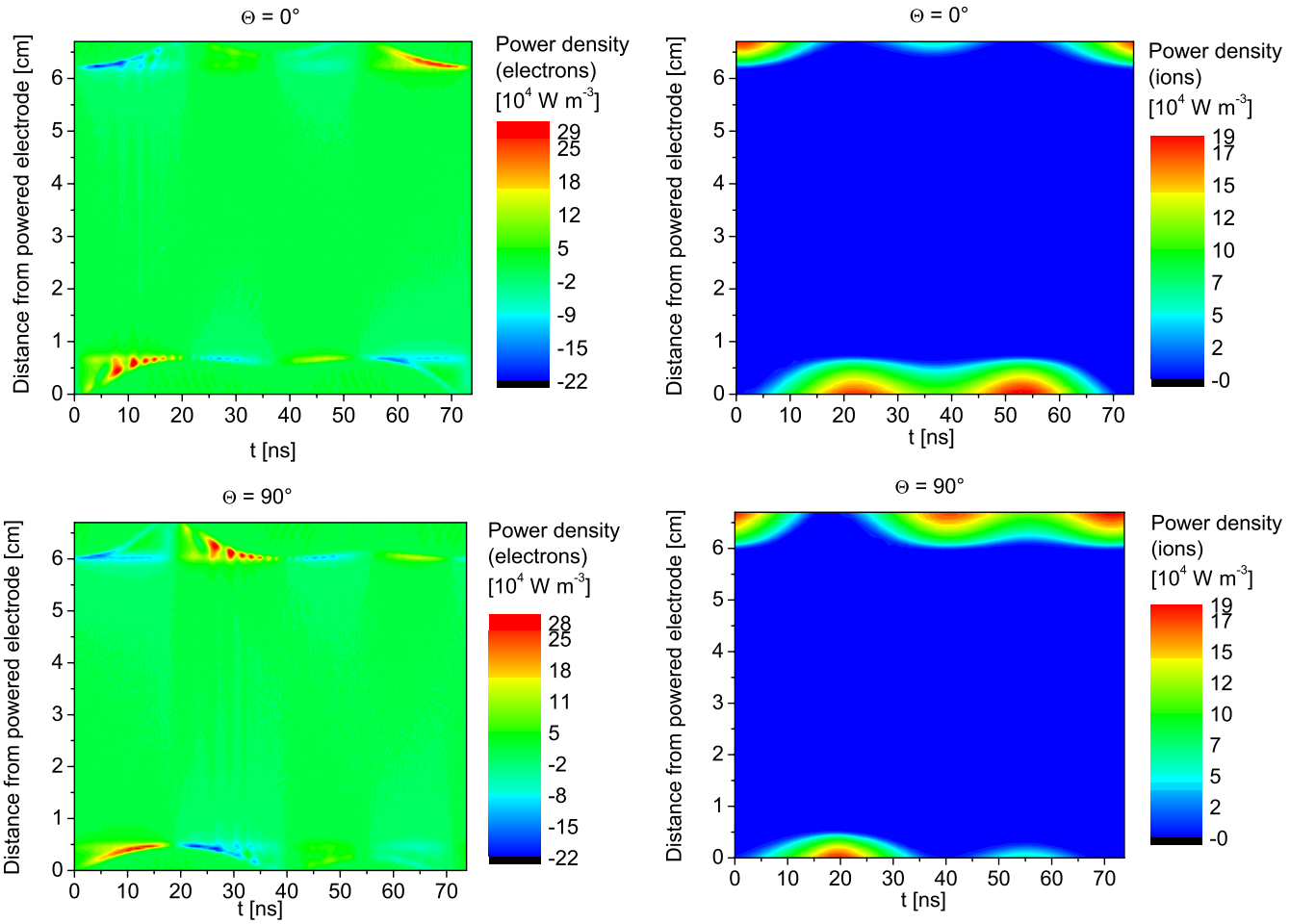

Figure 9. Spatio-temporal plots of the power density dissipated to electrons (left) and ions (right) at Θ = 0° (top) and Θ = 90° (bottom).

and the PSR effect cannot be observed. Before the EAE was discovered [1], it had been believed that the only way to make a discharge asymmetric is via changing the electrode sizes. However, via the EAE asymmetry can also be achieved electrically and, therefore, the PSR effect can be observed also in geometrically symmetric discharges.

Most of the power is absorbed by the ions, mainly inside the sheaths, where the ions are accelerated towards the electrodes by the strong sheath electric field.

For the PIC simulation the voltage is an input parameter and the voltage amplitude is kept constant. However, in experiments the applied power and not the voltage is usually

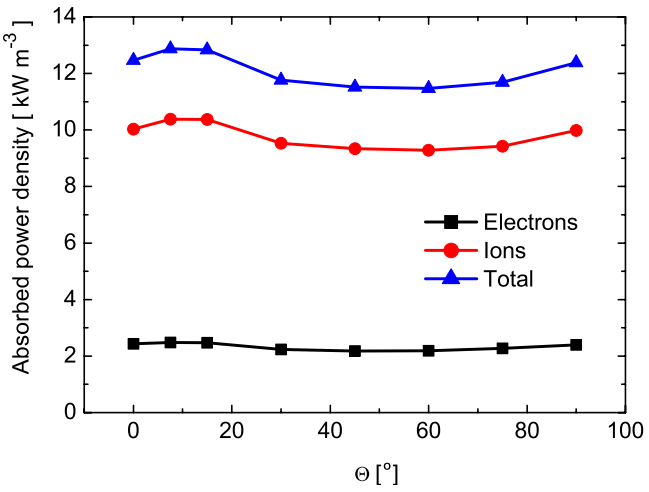

Figure 10. Power absorbed by electrons and ions and total power absorbed as a function of the phase angle Θ.

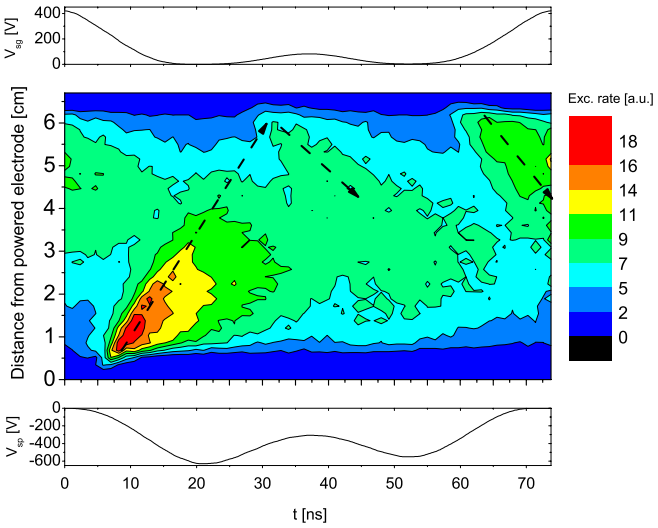

Figure 11. Spatio-temporal plot of the total excitation rate of argon atoms at $\Theta = 7.5^\circ$ calculated by the PIC simulation. The voltages across the sheath at the powered electrode, V_{sp}, and across the sheath at the grounded electrode, V_{sg}, are also shown.

set externally. Therefore, it is important to examine how the absorbed power changes as a function of Θ while the voltage amplitude is kept constant. The mean power density absorbed by electrons and ions, $\bar{p}_{e,i}$, results from an integration of the space and time resolved dissipated power density shown in figure 9:

$$\bar{p}_{e,i} = \frac{1}{d \cdot T_{lf}} \int_0^{T_{lf}} \int_0^d p_{e,i}\, dx\, dt. \qquad (11)$$

Here T_{lf} is the duration of one $1\,\omega$ RF period and d is the electrode gap. The results for the total dissipated power as well as the electron and ion components are shown in figure 10. The absorbed power density is essentially constant and does not differ from its mean value by more than about 6%. This means that keeping the applied voltage amplitude constant in the simulation corresponds to a good approximation to keeping the power constant. The small modulations of the absorbed power reflect the small modulations of the ion flux (figure 8). Therefore, the ion flux might change even less, if the power is kept constant.

The spatio-temporal total excitation rate of argon atoms at $\Theta = 7.5^\circ$ (phase of strongest dc self-bias) is shown in figure 11. The generation of beams of highly energetic electrons by the expanding sheath at both electrodes is observed. Such electron beams have been investigated experimentally and theoretically before [18–23, 25, 26, 45]. As the discharge is asymmetric at this phase angle (see figure 5), the sheath width and sheath expansion velocities are different at each electrode. Therefore [3, 4], the observed electron beams at each electrode are different. The strongest excitation is caused by the initial sheath expansion of the sheath at the powered electrode. These clearly visible beams have motivated the above hypothesis of a kinetic effect being responsible for the phase shift observed in the bias-phase relation. However, as already pointed out this issue requires a more detailed investigation.

3.2. Results with a 2 cm electrode gap at different pressures

In this section, results from PIC simulations are discussed for a gap of 2 cm and pressures of 4, 10 and 100 Pa, for voltages

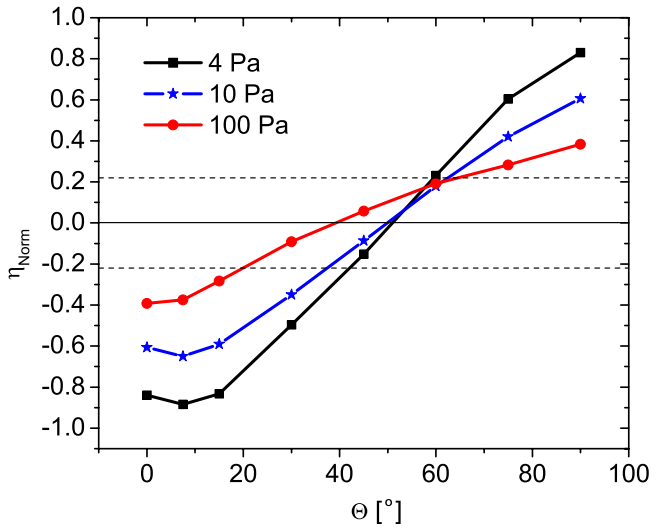

Figure 12. Dc self-bias normalized to the amplitude of the applied voltage as a function of the phase angle Θ at different pressures. The dashed lines correspond to the normalized bias $|\eta| = \frac{7}{32}$ resulting from the analytical model of [1] assuming $\varepsilon = 1$.

of 1000, 300 and 120 V. The conditions are otherwise the same as previously discussed.

Figure 12 shows the dc self-bias normalized to the amplitude of the applied voltage as a function of the phase angle Θ at different pressures. The strongest normalized bias $|\eta| = \frac{7}{32}$ resulting from the analytical model of [1] assuming $\varepsilon = 1$ is also shown (dashed lines). Obviously, the EAE is strongest at low pressures. At high pressures the normalized dc self-bias and, consequently, the degree of discharge asymmetry is smaller, since the self-amplification of the EAE vanishes with increasing pressure, because the sheath gets more collisional ($\varepsilon_{4\,Pa} \approx 0.6$, $\varepsilon_{10\,Pa} \approx 0.8$, $\varepsilon_{100\,Pa} \approx 1$ for $\Theta = 0^\circ$).

The ion flux-energy distributions resulting from the dc self-bias generated via the EAE at different pressures are

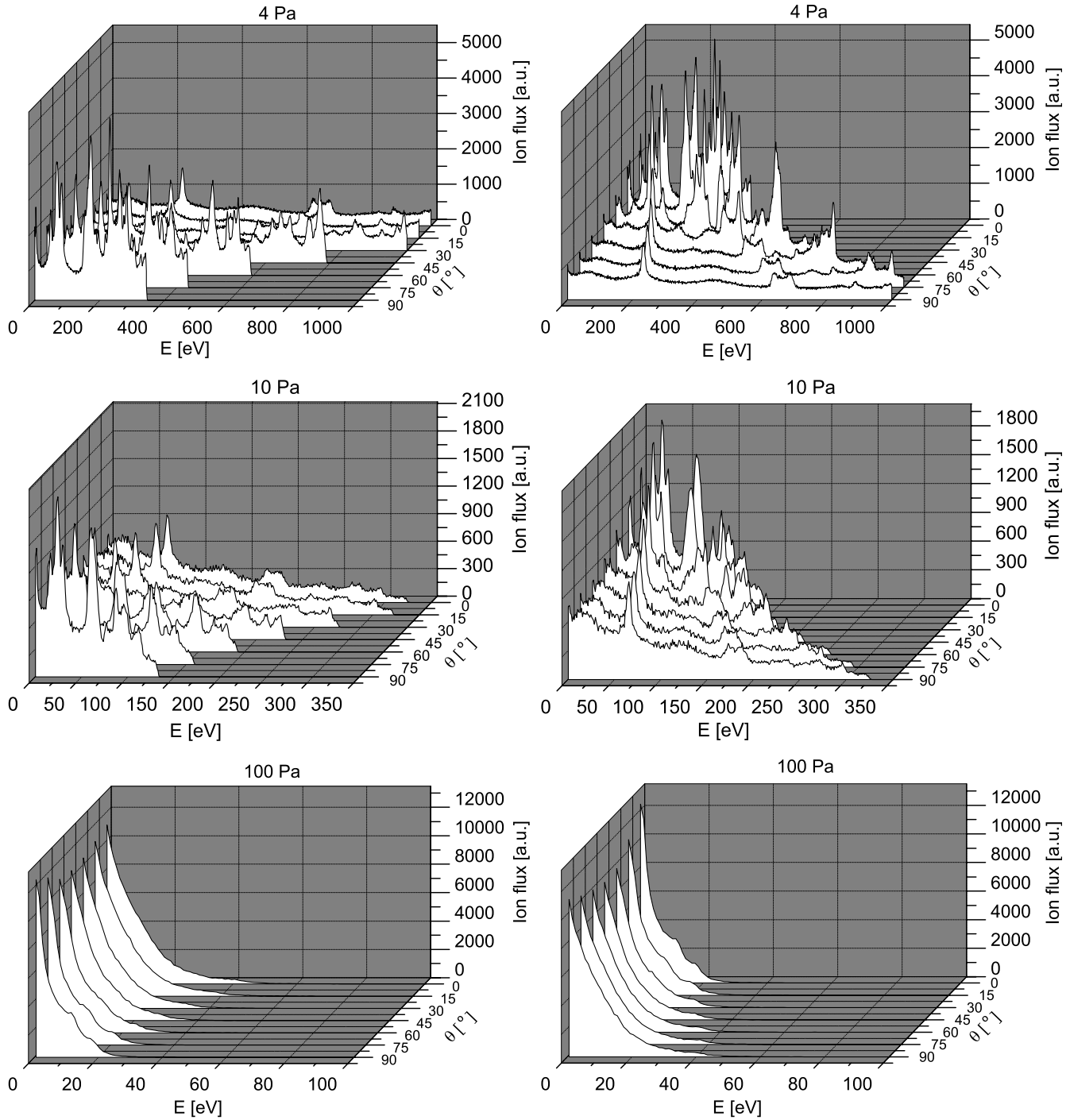

Figure 13. Ion flux-energy distributions at the powered (left column) and grounded (right column) electrodes as a function of the phase angle Θ at 4, 10 and 100 Pa for an electrode gap of 2 cm.

shown at each electrode in figure 13. The left column of figure 13 shows the ion flux-energy distributions at the indicated pressure at the powered electrode and the right column shows the ion flux-energy distributions at the grounded electrode. Due to the strong variable dc self-bias at low pressures of 4 and 10 Pa the maximum ion energy is changed by a factor of about 3 by changing the phase angle from 0° to 90°.

As discussed before, at the higher pressure of 100 Pa the dc self-bias is smaller. At 100 Pa the flux-energy distribution function is exponential. However, the mean ion energy can still be changed by tuning the phase angle. Figure 14 shows the mean ion energy $\langle \varepsilon_i \rangle$ as a function of the phase angle Θ at 100 Pa. The mean ion energy is changed by a factor of about 1.5 by tuning the phase from 0° to 90° at this pressure. The exponential form of the flux-energy distribution function is also well known from the dc case. There the mean ion energy in the highly collisional case (charge exchange) depends on the sheath voltage V and the sheath width s like V/s whereas s scales like $V^{3/5}$ [2]. For the energy this yields a rather weak scaling of $V^{2/5}$. This explains quite reasonably the observed moderate change in the ion energy in the 100 Pa case.

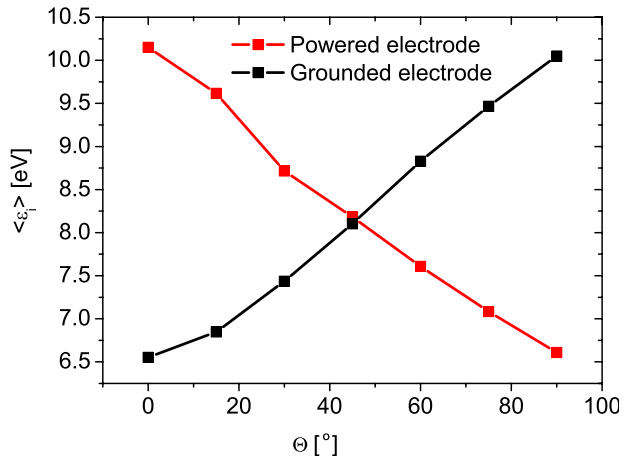

Figure 14. Mean ion energy as a function of the phase angle Θ at 100 Pa.

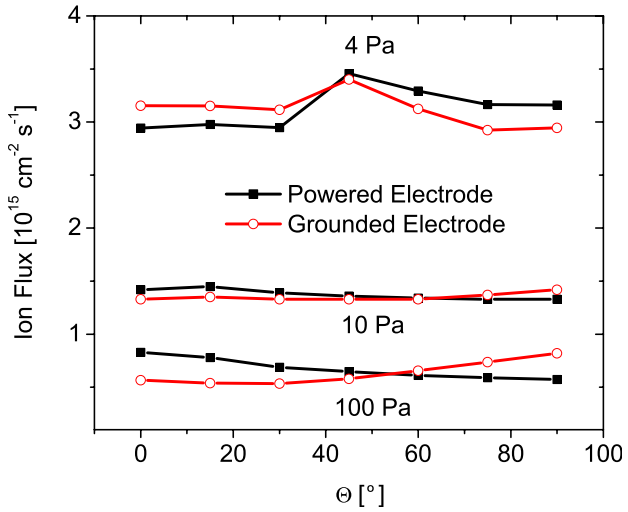

Figure 15. Ion flux as a function of the phase angle Θ at 4, 10 and 100 Pa for an electrode gap of 2 cm.

Figure 15 shows the ion flux as a function of the phase angle Θ. At the lower pressures of 4 and 10 Pa, when a strong dc self-bias is generated via the EAE (see figure 12) and the maximum ion energy is changed by a factor of 3 by changing the phase angle (see figure 13), the ion flux is constant within ±10%. At the higher pressure of 100 Pa the ion flux changes more significantly (±30%) and separate control of ion energy and flux is therefore limited. At higher pressures, secondary electrons become more important, since they are confined in the discharge volume and multiply themselves through ionization in the sheaths. The generation of secondary electrons is very sensitive to the sheath voltage and consequently also to the dc self-bias. Since the dc self-bias changes with Θ, ionization due to secondary electrons might also change with Θ.

4. Conclusions

The generation of a variable dc self-bias in geometrically symmetric dual-frequency CCRF discharges via the EAE was verified using a PIC simulation. As predicted by a previously developed fluid simulation and an analytical model [1], even in geometrically symmetric CCRF discharges the two sheaths are no longer symmetric, if the RF voltage waveform applied to a CCRF discharge contains an even harmonic of the fundamental frequency. However, this does not necessarily yield different mean sheath voltages and mean ion energies. In fact, the phase angle between the fundamental and the even harmonic is the essential parameter for controlling the asymmetry between these quantities: the symmetry of the applied voltage waveform can be changed from symmetric to antisymmetric and vice versa by changing the phase between the fundamental and its even harmonic. If the absolute values of the positive and negative extremes of the applied voltage waveform are different, a dc self-bias will develop in order to balance electron and ion fluxes at each electrode. This bias causes the mean sheath voltages and, consequently, the mean ion densities in both sheaths to be different. This enhances the degree of discharge asymmetry and self-amplifies the effect. The self-bias and, consequently, the ion energy can be controlled by tuning the phase angle, while the ion flux stays approximately constant. The effect is maximized by applying the second harmonic of the fundamental to the discharge as second frequency.

Under the conditions used in [1] the dc self-bias in a low pressure argon discharge operated at 13.56 and 27.12 MHz is calculated in dependence of the phase between the two applied RF voltage waveforms. In agreement with previous results the dc self-bias is found to be a nearly linear function of the phase angle. A small phase shift of about 7° is found between the fluid dynamic simulation and the analytical model on the one hand and the PIC results on the other hand. This shift might be related to a kinetic effect, but this remains the subject of ongoing investigations so far.

The effect of this variable dc self-bias on the ion flux-energy distribution at each electrode is investigated. The maximum ion energy at the electrode surface is changed by a factor of 3 by changing the phase angle from 0° to 90°. Furthermore, the role of the electrodes can be reversed electrically by changing the phase angle.

The effect of the phase variation on the ion flux and plasma density is investigated. The ion flux is found to be constant within ±5% when changing the phase angle. This result in combination with the opportunity to change the maximum ion energy by a factor of 3 by changing the phase angle clearly shows that separate control of the ion flux and ion energy can be achieved in an almost ideal way via the EAE.

This result is particularly interesting for industrial applications, since it allows efficient separate control of ion flux and energy using an easily applied technique. In many cases existing process chambers could be easily modified to make use of the EAE by simply replacing the matching and power supply. Using this technique reactor sizes and, consequently, costs can be reduced, since high area ratios are no longer needed. Furthermore, limitations of the separate control of ion flux and energy by frequency coupling in conventional dual-frequency CCRF discharges operated at substantially different frequencies can be avoided.

Before it was assumed that the PSR effect can only be observed in geometrically asymmetric discharges.

However, due to the EAE the PSR effect is observed for the first time in a simulation of a geometrically symmetric discharge in terms of high frequency modulations of the power density dissipated to the electrons in this work, since even in geometrically symmetric discharges the two sheaths can be made asymmetric electrically via the EAE.

The EAE has been studied at different pressures and electrode gaps. At relatively low pressures below 100 Pa efficient separate control of ion energy and flux can be achieved via the EAE. The regime of efficient separate control corresponds to conditions most relevant for industrial applications.

A method for controlling the ion energy based upon this effect is patent pending (PCT application No PCT/EP2008/059133).

Acknowledgments

This work has been funded by the DFG through GRK 1051, the Ruhr University Research School and the Hungarian Scientific Research Fund through grants OTKA-T-48389 and OTKA-IN-69892.

References

[1] Heil B G, Czarnetzki U, Brinkmann R P and Mussenbrock T 2008 *J. Phys. D: Appl. Phys.* **41** 165202
[2] Lieberman M A and Lichtenberg A J 2005 *Principles of Plasma Discharges and Materials Processing* 2nd edn (New Jersey: Wiley Interscience)
[3] Lieberman M A 1988 *IEEE Trans. on Plasma Sci.* **16** 638
[4] Lieberman M A and Godyak V A 1998 *IEEE Trans. Plasma Sci.* **26** 955
[5] Surendra M and Graves D B 1991 *Phys. Rev. Lett.* **66** 1469
[6] Turner M M 1995 *Phys. Rev. Lett.* **75** 1312
[7] Gozadinos G, Turner M M and Vender D 1995 *Phys. Rev. Lett.* **87** 135004
[8] Kaganovich I D 2002 *Phys. Rev. Lett.* **89** 265006
[9] Kaganovich I D, Polomarov O V and Theodosioue C E 2006 *IEEE Trans. Plasma Sci.* **34** 696
[10] Klick M 1996 *J. Appl. Phys.* **79** 3445
[11] Klick M, Kammeyer M, Rehak W, Kasper W, Awakowicz P and Franz G 1998 *Surf. Coat. Technol.* **98** 1395
[12] Mussenbrock T and Brinkmann R P 2006 *Appl. Phys. Lett.* **88** 151503
[13] Mussenbrock T and Brinkmann R P 2007 *Plasma Sources Sci. Technol.* **16** 377–85
[14] Czarnetzki U, Mussenbrock T and Brinkmann R P 2006 *Phys. Plasmas* **13** 123503
[15] Lieberman M A, Lichtenberg A J, Kawamura E, Mussenbrock T and Brinkmann R P 2008 *Phys. Plasmas* **15** 063505
[16] Mussenbrock T, Brinkmann R P, Lieberman M A, Lichtenberg A J and Kawamura E 2008 *Phys. Rev. Lett.* **101** 085004
[17] Ziegler D, Mussenbrock T and Brinkmann R P 2008 *Plasma Sources Sci. Technol.* **17** 045011
[18] Schulze J, Heil B G, Luggenhölscher D, Mussenbrock T, Brinkmann R P and Czarnetzki U 2008 *J. Phys. D: Appl. Phys.* **41** 042003 (FTC)
[19] Schulze J, Heil B G, Luggenhölscher D, Brinkmann R P and Czarnetzki U 2008 *J. Phys. D: Appl. Phys.* **41** 195212
[20] Schulze J, Donkó Z, Heil B G, Luggenhölscher D, Mussenbrock T, Brinkmann R P and Czarnetzki U 2008 *J. Phys. D: Appl. Phys.* **41** 105214
[21] Schulze J, Kampschulte T, Luggenhölscher D and Czarnetzki U 2007 *J. Phys. Conf. Ser.* **86** 012010
[22] Schulze J, Heil B G, Luggenhölscher D and Czarnetzki U 2008 *IEEE Trans. Plasma Sci.* **36** 1400
[23] Heil B G, Schulze J, Mussenbrock T, Brinkmann R P and Czarnetzki U 2008 *IEEE Trans. Plasma Sci.* **36** 1404
[24] Salabas A, Marques L, Jolly J and Alves L L 2004 *J. Appl. Phys.* **95** 4605–20
[25] Vender D and Boswell R W 1990 *IEEE Trans. Plasma Sci.* **18** 725
[26] Wood B P 1991 *PhD Thesis* University of California at Berkely
[27] Tochikubo F, Suzuki A, Kakuta S, Terazono Y and Makabe T 1990 *J. Appl. Phys.* **68** 5532
[28] Petrović Z Lj, Tochikubo F, Kakuta S and Makabe T 1992 *J. Appl. Phys.* **71** 2143
[29] Czarnetzki U, Luggenhölscher D and Döbele H F 1999 *Plasma Sources Sci. Technol.* **8** 230
[30] Gans T, Schulz-von der Gathen V and Döbele H F 2004 *Europhys. Lett.* **66** 232
[31] Belenguer Ph and Boeuf J P 1990 *Phys. Rev.* A **41** 4447
[32] Sato A H and Lieberman M A 1990 *J. Appl. Phys.* **68** 6117
[33] Vender D and Boswell R W 1992 *J. Vac. Sci. Technol.* A **10** 1331
[34] Turner M M and Hopkins M B 1992 *Phys. Rev. Lett.* **69** 3511
[35] Rauf S and Kushner M J 1999 *IEEE Trans. Plasma Sci.* **27** 1329
[36] Boyle P C, Ellingboe A R and Turner M M 2004 *Plasma Sources Sci. Technol.* **13** 493–503
[37] Boyle P C, Ellingboe A R and Turner M M 2004 *J. Phys. D: Appl. Phys.* **37** 697
[38] Kitajima T, Takeo Y, Petrovic Z L and Makabe T 2000 *Appl. Phys. Lett.* **77** 489
[39] Denda T, Miyoshi Y, Komukai Y, Goto T, Petrovic Z L and Makabe T 2004 *J. Appl. Phys.* **95** 870
[40] Lee J K, Manuilenko O V, Babaeva N Yu, Kim H C and Shon J W 2005 *Plasma Sources Sci. Technol.* **14** 89
[41] Kawamura E, Lieberman M A and Lichtenberg A J 2006 *Phys. Plasmas* **13** 053506
[42] Turner M M and Chabert P 2006 *Phys. Rev. Lett.* **96** 205001
[43] Gans T, Schulze J, O'Connell D, Czarnetzki U, Faulkner R, Ellingboe A R and Turner M M 2006 *Appl. Phys. Lett.* **89** 261502
[44] Schulze J, Gans T, O'Connell D, Czarnetzki U, Ellingboe A R and Turner M M 2007 *J. Phys. D: Appl. Phys.* **40** 7008–18
[45] Schulze J, Donkó Z, Luggenhölscher D and Czarnetzki U 2008 *Plasma Sources Sci. Technol.* submitted
[46] Semmler E, Awakowicz P and von Keudell A 2007 *Plasma Sources Sci. Technol.* **16** 839
[47] Salabas A and Brinkmann R P 2005 *Plasma Sources Sci. Technol.* **14** S53–9
[48] Donkó Z and Petrović Z Lj 2006 *Japan. J. Appl. Phys.* **45** 8151
[49] Donkó Z and Petrović Z Lj 2007 *J. Phys.: Conf. Series* **86** 012011
[50] Phelps A V and Petrović Z Lj 1999 *Plasma Sources Sci. Technol.* **8** R21
[51] Phelps A V 1994 *J. Appl. Phys.* **76** 747
[52] Phelps A V http://jilawww.colorado.edu/~avp/collision_data/ unpublished
[53] Godyak V A, Piejak R B and Alexandrovich B M 1992 *Plasma Sources Sci. Technol.* **1** 36
[54] Heil B G, Brinkmann R P and Czarnetzki U 2008 *J. Phys. D: Appl. Phys.* **41** 225208
[55] Brinkmann R P 2007 *J. Appl. Phys.* **102** 093303
[56] Tsuboi H, Itoh M, Tanabe M, Hayashi T and Uchida T 1995 *Japan. J. Appl. Phys.* **34** 2476
[57] Chinzei Y, Ogata M, Sunada T, Itoh M, Hayashi T, Shindo H, Itatani R, Ichiki T and Horiike Y 1999 *Japan. J. Appl. Phys.* **37** 4572